East-Frisian Wadden Sea hydrodynamics and wave propagation in an unstructured-grid model

Sebastian Grashorn[1], Karsten A. Lettmann[2], Jörg-Olaf Wolff[2], Thomas H. Badewien[2], Emil Stanev[1]

Abstract

An unstructured-grid model (FVCOM) coupled to a wave model (FVCOM-SWAVE) with two different setups with different grid resolutions is used to investigate the hydrodynamic and wave energy conditions during a moderate and a storm situation in this area. The results of both model setups are validated, compared to each other and analysed with a focus on longshore currents, radiation stress effects and wave energy. The modelled longshore currents are compared with two theoretical approaches for the expected magnitude of the wave-induced longshore current. Model results show that during storm conditions strong alongshore currents occur in front of the barrier islands with speeds around 1 m/s reaching even higher values with higher grid resolution and wave energies have values of up to 190 kW/m.

Key words: Numerical modelling, FVCOM, Wave-current interactions, Longshore currents, Wave energy, Wadden Sea

1. Introduction

The German coast located in the area of the southern part of the North Sea has been exposed to storm surges and resultant floodings since hundreds of years. Hence, people living close to the coast tried to adapt themselves and their environment to prevent damage caused by extreme storm conditions and extreme sea levels. Extreme sea levels can be caused by high astronomical tides, storm surges, wind-generated gravity waves at the surface of the ocean, swells or a changing sea level (see Weisse et al., 2012). Especially considering climate change and sea level rise, future storm events might be even more destructive compared to the past. The barrier island system of the Dutch and German Wadden Sea including various tidal inlets has been subject to many studies focusing on different features of this unique coastal system. Dastgheib et al. (2008), Van der Wegen et al. (2010) and Yu et al. (2012) used models to investigate aspects of the long-term morphological evolution of tidal inlet areas. In the East Frisian Wadden Sea Stanev et al. (2003ab, 2007a) and Staneva et al. (2009) used numerical modelling tools and observation data to describe different physical aspects of the hydrodynamics in this area. Stanev et al. (2006) and Stanev et al. (2007b) investigated driving factors of sediment dynamics and Lettmann et al. (2009) focused on the dynamical response of sediment dynamics for different scenarios including storm conditions using numerical modelling. Reuter et al. (2009) and Bartholomä et al. (2009) used measuring results to investigate similar aspects. Most of these papers come to the conclusion that the East-Frisian Wadden Sea inlets are ebb-dominated. Stanev et al. (2003a) also analysed the water transport and turbulence patterns inside this area to account for the possibility of a net sediment export/import.

The impact of wave energy generated by wind on the coast and the currents in the area of the East-Frisian Wadden Sea has been investigated in this contribution. A similar study for the area around the northern Frisian Wadden Sea barrier island Sylt is given by Pleskachevsky et al. (2009). In another study for the Ems-Dollard estuary within the KLIFF project, Weisse et al. (2012) reported that they found indicators that the present coastal protection strategies will work even under changing climate conditions and that no general change in strategy is required at least for the coming decades.

The effects of wave-current interactions caused by radiation stress have been subject to several publications (see e.g. Longuet-Higgins, 1970; Thornton and Guza, 1986; Osuna and Monbaliu, 2004;

[1]Institute of Coastal Research, Helmholtz-Zentrum Geesthacht Centre for Materials and Coastal Research (HZG), Max-Planck-Str. 1, 21502 Geesthacht, Germany. sebastian.grashorn@hzg.de, emil.stanev@hzg.de

[2]Institute for Chemistry and Biology of the Marine Environment (ICBM), Carl von Ossietzky Universität Oldenburg, Carl-von-Ossietzky-Str. 9-11, 26111 Oldenburg, Germany. lettmann@icbm.de, wolff@icbm.de, badewien@icbm.de

Pleskachevsky et al., 2009). Longuet-Higgins (1970) and Thornton and Guza (1986) derived equations for the magnitude of the longshore current. Pleskachevsky et al. (2009) investigated the impact of a storm surge on the North-Frisian island of Sylt by estimating the wave energy flux and the effects of wave-current interactions. Using a two-way-coupled modelling system they found that a wave-induced current of 1 m/s and a wave energy flux of about 160 kW/m can be estimated in their area of interest. Osuna and Monbaliu (2004) investigated various aspects of wave-current interactions with a focus on the Belgian coast.

An application of an unstructured-grid model that is two-way-coupled to a surface wave model with a high resolution of up to 50 m in the area of the chain of barrier islands in the East-Frisian Wadden Sea to investigate the wave-induced longshore currents and the energy flux along the coast has not been the focus of a study yet. In this contribution, the three dimensional, unstructured grid modelling system FVCOM (see Chen et al., 2003; Qi et al., 2009), which is a "combination" of the hydrodynamic model FVCOM and the wave model FVCOM-SWAVE, is used. This modelling system is applied to the North Sea and the chain of the barrier islands in the East-Frisian Wadden Sea using two setups with a high resolution in regions of high interest and with a reduced resolution towards the open North Sea.

The study presented in this contribution aims to (i) test and discuss the usage and reliability of an unstructured-grid ocean model in the North Sea and the East Frisian Wadden Sea; (ii) compare the results given by a coarse North Sea model and a highly resolved Wadden Sea model; (iii) discuss the effects of the wave-current interaction and the wave energy input at the East-Frisian Wadden Sea coast for moderate and storm conditions.

2. Study site

The study site is located in the southern part of the North Sea including a W-E oriented chain of barrier islands and the northwestern coast of Germany (see figure 1). In this area several tidal flats and basins can be found between the islands and the coast, which are connected to the deeper sea via tidal channels. A tidal amplitude of 1.5 m is reached during spring tides and of 1.0 m during neap tides (see Lettmann et al. 2009) and thus the area can be identified as a meso tidal zone (see Flemming and Bartholomä, 1997; Stanev et al., 2003a). The current velocity can reach a maximum of 1.5 m/s in the channels (see Santamarina Cuneo and Flemming, 2000). Krögel and Flemming (1998) summarise that the energy flux in the tidal catchment is controlled by the tidal currents, waves generated in the tidal basins and swells entering the inlet from the open North Sea. Most of the energy transported by the swells is dissipated at the ebb delta and only 10 % of the energy is penetrating the inlet. The region is dominated in 2005 by westerly winds (occurrence about 72 %) with winds coming from the NW- and SW-direction accounting for 36% each over the year (see Loewe, 2009). At the ICBM pile station the mean significant wave height was only about 0.36 m during Dec. 2006 until June 2007. This indicates that the chain of barrier island decreases the wave energy reaching the coast of the mainland enormously (see Lettmann et al., 2009).

3. Model

3.1. *Model description*

The computations were performed with the modelling system FVCOM, version 3.1.4. The Fortran-based FVCOM is a prognostic, unstructured-grid, finite-volume, free-surface, 3D primitive equations ocean model that was originally developed by Chen et al. (2003). The model solves the integral form of the governing equations for momentum, continuity, temperature, salinity and density by calculating the fluxes over a triangular mesh composed of non-overlapping horizontal control volumes using spherical coordinates (see manual provided by Chen et al. 2006). This can be done in a 2D-mode with vertical integrated equations and in a 3D-mode. Tracers like e.g. temperature, salinity or surface elevation are calculated on each node of the unstructured triangles while the velocities are calculated at the center of a triangle by the net flux through the three sides of that triangle.

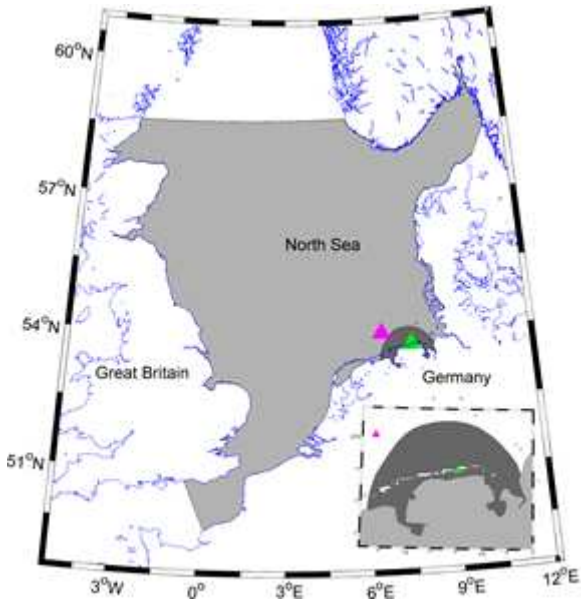

Figure 1. Area of interest including the North Sea and the German Bight. The two gray shaded areas depict the coverage of the North Sea and the high-resolution Wadden Sea model. A zoom into the area of the East-Frisian Wadden Sea can be seen in the lower right corner of the picture. The magenta-coloured triangle shows the position of the FINO I pile station and the green triangle shows the position of the ICBM pile station.

The governing equations used by FVCOM are summarised by Wu et al. (2011) and were derived by Mellor (2003, 2005, 2008) in sigma coordinates as follows:

$$\frac{\partial uD}{\partial t}+\frac{\partial u^2 D}{\partial x}+\frac{\partial uvD}{\partial y}+\frac{\partial uw}{\partial \sigma}-fvD = -D\frac{\partial}{\partial x}(g\hat{\eta}+p_{atm})-D\int_{\sigma}^{0}\left(D\frac{\partial b}{\partial x}-\sigma\frac{\partial D}{\partial x}\frac{\partial b}{\partial \sigma}\right)d\sigma - \left(\frac{\partial DS_{xx}}{\partial x}+\frac{\partial DS_{xy}}{\partial y}\right)+\sigma\left(\frac{\partial D}{\partial x}\frac{\partial S_{xx}}{\partial \sigma}+\frac{\partial D}{\partial y}\frac{\partial S_{xy}}{\partial \sigma}\right)+\frac{\partial \tau_x}{\partial \sigma} \tag{2}$$

$$\frac{\partial vD}{\partial t}+\frac{\partial uvD}{\partial x}+\frac{\partial v^2 D}{\partial y}+\frac{\partial vw}{\partial \sigma}+fuD = -D\frac{\partial}{\partial y}(g\hat{\eta}+p_{atm})-D\int_{\sigma}^{0}\left(D\frac{\partial b}{\partial y}-\sigma\frac{\partial D}{\partial y}\frac{\partial b}{\partial \sigma}\right)d\sigma - \left(\frac{\partial DS_{xy}}{\partial x}+\frac{\partial DS_{yy}}{\partial y}\right)+\sigma\left(\frac{\partial D}{\partial x}\frac{\partial S_{xy}}{\partial \sigma}+\frac{\partial D}{\partial y}\frac{\partial S_{yy}}{\partial \sigma}\right)+\frac{\partial \tau_y}{\partial \sigma} \tag{3}$$

$$\frac{\partial Du}{\partial x}+\frac{\partial Dv}{\partial y}+\frac{\partial \omega}{\partial \sigma}+\frac{\partial \hat{\eta}}{\partial t}=0 \tag{4}$$

$$\frac{\partial \Theta D}{\partial t}+\frac{\partial \Theta uD}{\partial x}+\frac{\partial \Theta vD}{\partial y}+\frac{\partial \Theta \omega}{\partial \sigma}=\frac{1}{D}\frac{\partial}{\partial \sigma}\left(K_h\frac{\partial \Theta}{\partial \sigma}\right)+D\hat{H}+DF_{\Theta} \tag{5}$$

$$\frac{\partial sD}{\partial t}+\frac{\partial suD}{\partial x}+\frac{\partial svD}{\partial y}+\frac{\partial s\omega}{\partial \sigma}=\frac{1}{D}\frac{\partial}{\partial \sigma}\left(K_h\frac{\partial s}{\partial \sigma}\right)+DF_s \tag{6}$$

$$\rho=\rho(\Theta,s) \tag{7}$$

Here, x and y are the cartesian east and north directions respectively, and $\sigma=\frac{z-\eta}{D}=\frac{z+H}{D}-1$ is the vertical terrain-following sigma-coordinate; u and v are the corresponding components of the velocities in the x- and y-direction and ω is the velocity normal to the sigma surfaces that has to be set to 0 at the surface and the bottom of the water column (see Mellor, 2008); τ_x and τ_y are the corresponding components of the wind stress; $\hat{\eta}$ is the mean surface elevation; h is the mean water depth; D = h+ $\hat{\eta}$ is the total water depth; Θ the potential temperature; s the salinity; ρ is the density; p_{atm} is the air pressure; b is the buoyancy; f is the Coriolis parameter; $\hat{H}$ is the solar irradiance; K_h is the thermal vertical eddy diffusion coefficient; F_Θ and F_s represent the thermal and salt diffusion terms. The modified Mellor and Yamada level 2.5 (MY-2.5) and Smagorinsky turbulent closure schemes are utilised as default setups for vertical and horizontal mixing, respectively (see Mellor and Yamada 1982; Smagorinsky 1963; Wu et al. 2011). S_{xx}, S_{xy} and S_{yy} are the radiation stress terms that describe the wave-current interaction and are defined by Mellor (2008) as

$$S_{xx}=kE\left(\frac{k_x^2}{k^2}F_{CS}F_{CC}-F_{SC}F_{SS}\right)+E_D \tag{8}$$

$$S_{yy}=kE\left(\frac{k_y^2}{k^2}F_{CS}F_{CC}-F_{SC}F_{SS}\right)+E_D \tag{9}$$

$$S_{xy}=S_{yx}=kE\frac{k_xk_y}{k^2}F_{CS}F_{CC} \tag{10}$$

with the wave energy E (see Mellor, 2008; Wu et al., 2011) that can be seen as the sum of the kinetic and the potential wave energies (see Mellor, 2003) and

$$E=\frac{1}{2}ga^2=\frac{1}{16}gH_s^2 \tag{11}$$

$$E_D=0 \; if \; z\neq\hat{\eta} \; and \int_{-h}^{\hat{\eta}+\tilde{\eta}}E_D dz=E/2. \tag{12}$$

Here, k_x, k_y and k are the wave number in x-direction, in y-direction and the absolute wave number, respectively, H_s is the significant wave height and $\tilde{\eta}$ is the surface elevation caused by the wind-generated waves. The terms F_{ss}, F_{sc}, F_{cs} and F_{cc} are defined as follows (see Mellor, 2008):

$$F_{SS}\equiv\frac{\sinh k(z+h)}{\sinh kD} \tag{13}$$

$$F_{SC}\equiv\frac{\sinh k(z+h)}{\cosh kD} \tag{14}$$

$$F_{SS}\equiv\frac{\cosh k(z+h)}{\sinh kD} \tag{15}$$

$$F_{CC}\equiv\frac{\cosh k(z+h)}{\cosh kD} \tag{16}$$

In order to provide a sufficient representation of an irregular topography vertically a σ-coordinate system is used. The vertical velocity is placed at the surface of the σ-layer while all other variables are

calculated at the mid-level of a layer. FVCOM allows the user to use either uniform or non-uniform σ-layers.

The 2D third-generation structured-grid surface wave model SWAN (see Booij et al., 1999) has been added to the original source code of FVCOM as an unstructured-grid finite-volume version named FVCOM-SWAVE (see Qi et al., 2009) for the use in coastal ocean regions with a complex irregular geometry. The resultant modelling system can be applied to investigate the influence of wave energy generated by wind on the coast and the wave-induced currents.

FVCOM-SWAVE was utilised in a non-stationary mode with a time step of 300 s for the North Sea model and a time step of 10 s for the Wadden Sea model. The default conditions for wave energy input and dissipation and for wave propagation were applied. In detail, the processes of wave growth, quadruplet wave interactions, white capping, wave breaking, bottom friction and triad wave interactions have been activated.

For FVCOM a time step of 10 s for the North Sea model and a time step of 2 s for the Wadden Sea model were used. The salinity and the temperature were set to a constant value of 35 PSU and 10 °C, respectively. To use this approach might be justified by the fact that during the investigated period in autumn density gradients in the Wadden Sea show a seasonal minimum (see Wang et al. 2011). The default values for bottom friction and vertical and horizontal mixing were applied.

The computations were performed on the cluster of the North-German Supercomputing Alliance (Norddeutscher Verbund zur Förderung des Hoch- und Höchstleistungsrechnens - HLRN) and the cluster HERO (High-End Computing Resource Oldenburg), funded by the Deutsche Forschungsgemeinschaft (DFG) and the Ministry of Science and Culture (MWK) of the State of Lower Saxony, Germany.

3.2. *Model topography and surface wind and pressure forcing*

The digital topography of the East Frisian Wadden Sea is a combination of high-resolution data provided by the BSH and the NLWKN (Niedersächsischer Landesbetrieb für Wasserwirtschaft, Küsten- und Naturschutz). The topography data for the deeper North Sea were taken from the ETOPO2 (U.S. Department of Commerce, National Oceanic and Atmospheric Administration, National Geophysical Data Center, 2006. 2-minute Gridded Global Relief Data (ETOPO2v2)) data set (see Lettmann et al., 2009). The coastline was extracted from the commercial software Cruising Navigator distributed by Maptech Inc. and combined with the extracted coastline from the NOAA National Geophysical Data Center (WVS) (http://www.ngdc.noaa.gov/mgg/shorelines/shorelines.html). The wind and pressure data was provided by the DWD (German Weather Service) with a temporal resolution of 1h in 2006 and 2h in 2007.

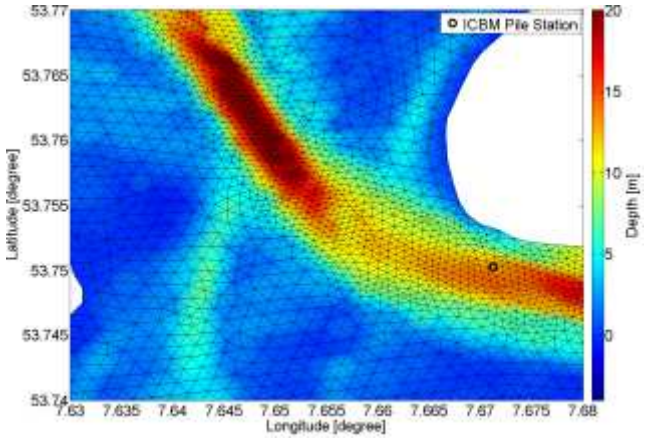

Figure 2. Tidal channel between the barrier islands Langeoog and Spiekeroog. The mesh resolution is increased to 50 m here.

3.3. *Mesh generation*

FVCOM does not include a mesh generating system, so a freely available finite element mesh generator called GMSH has been utilised (see Geuzaine and Remacle, 2009). With this tool the resolution of the mesh can be increased in areas of interest. For this study the mesh resolution has been increased in the area of the tidal channels in between the barrier islands because high current velocities are known to occur there.

Before a mesh can be generated, a coastline and topography data has to be provided by the user. The generated mesh has been improved regarding to some empirical quality criteria. The following criteria have been applied (see manual given by Chen et al., 2006):

1. The minimum interior angle must be greater than 30 degrees.
2. The maximum interior angle must be less than 130 degrees.
3. The area change of adjacent triangles must be less than a factor of 2.

Figure 2 shows a section of the mesh that is used for the investigation of the wave-current interactions in the area of the East-Frisian Wadden Sea.

The resolution of the coastline and inside the model area close to the area of interest is 120 m. It is reduced to 300 m and 500 m in an intermediate zone and finally to 2000 m in the region close to the boundary of the model. In the tidal channels the resolution is 50 m in order to resolve higher dynamics sufficiently (see figure 2).

3.4. *Surface and wave forcing at the open boundaries*

The modelling system FVCOM-SWAVE provides the opportunity to force the model at the open boundary using a predetermined surface elevation and/or wave conditions. For the surface elevation at the three open boundaries (see figure 1) of the North Sea model the output of the Global Tide model FES2004 (Finite Element Solution 2004) was used. FES99 (FES2004) was produced by Legos and CLS Space Oceanography Division and distributed by Aviso, with support from CNES (http://www.aviso.oceanobs.com) (see Lyard et al., 2006). The surface elevation is affected by the inverse barometer effect, such that a change of 1 hPa will result in a change of 1 cm in surface elevation (see Kliem et al., 2006). This correction was applied to the FES2004 output data.

A southward-directed JONSWAP wave spectrum (see Holthuijsen, 2007) with a significant wave height of 1 m and a peak period of 10 s is defined as a boundary condition in the FVCOM-SWAVE input file for the North Sea setup.

The Wadden Sea model is one-way nested in the North Sea model, thus providing the surface elevation and wave conditions for the open boundary forcing of the highly resolved model. The peak period at the boundary had to be smoothed to guarantee a stable model run.

4. Validation and comparison of the model results

For validation purposes of the model two time periods in 2006 and 2007 were analysed for the North Sea and the Wadden Sea model.

In figure 3 the calculated and measured significant wave height, peak period and wave direction in Oct./Nov. 2006 and Nov. 2007 at the FINO I pile station (see figure 1) can be seen. The mean significant wave height in 2007 is around 3 m, but during a storm event in 2006 it can go up to more than 9 m. During the storm period, the model seems to reproduce the measured significant wave height, peak period and wave direction reasonably. It can also be seen that in 2006 and 2007 the main wave directions are N-NW and the main peak period is about 7 s in 2007, but it can go up to 14 s during the storm event in 2006.

A vertical distribution of the current velocity at the ICBM pile station (see figure 1) can be seen in figure 4. The North Sea model clearly underestimates the current velocity, but the Wadden Sea model shows reasonably results. However, both models cannot reproduce short time fluctuations of the current velocity.

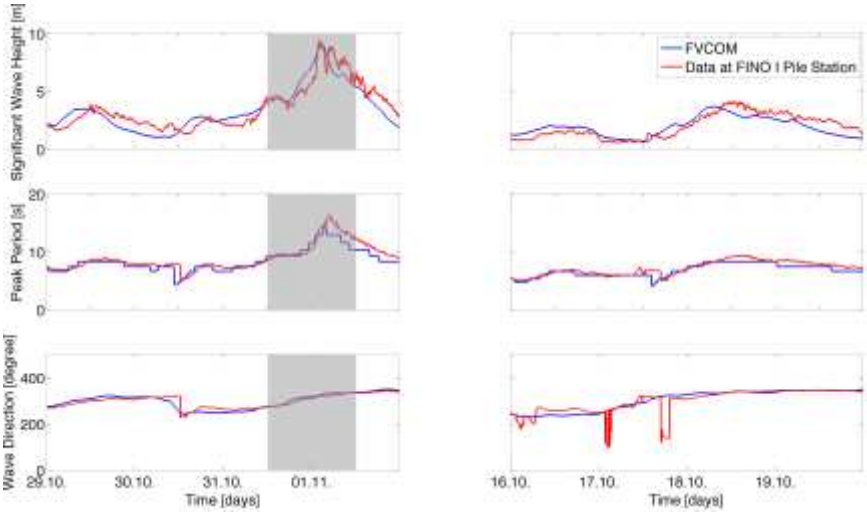

Figure 3. Measured and modelled significant wave height, peak period and wave direction at the FINO I pile station calculated with the North Sea setup. On the left hand the time period 29.10.06-02.11.06 including the storm surge Britta (grey colour) is shown. On the right hand the time period 16.10.07-20.10.07 is shown.

5. Radiation stress effects

Longuet-Higgins and Stewart (1964) described an effect they called radiation stress and calculated this term as the phase-averaged depth-integrated flux of horizontal momentum caused by a harmonic one-directional wave traveling in the x-direction (see also Longuet-Higgins, 1970):

$$\left\langle \int_{-h}^{\xi} \left(p + \rho u^2\right) dz \right\rangle - \int_{-h}^{0} p_0 dz = E\left(\frac{2kh}{\sinh 2kh} + \frac{1}{2}\right) \tag{17}$$

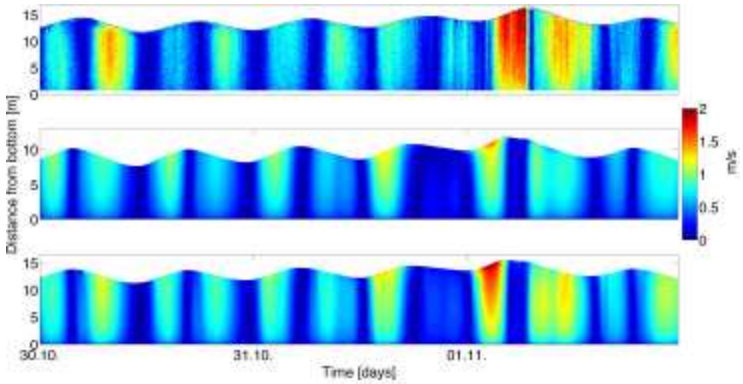

Figure 4. Measured and modelled current velocity at the ICBM pile station between two barrier islands between the 30.10.06 and 02.11.06. The top panel shows the measured data. In the middle panel the result of the North Sea model and in the bottom panel the result of the Wadden Sea model can be seen.

Here, ξ, h, p, p_0, ρ, u, E and k are the surface elevation, depth, wave-induced pressure, hydrostatic pressure, water density, particle velocity in x-direction, energy density and wave number, respectively. The term ρu^2 describes the transport of momentum at a rate u per unit time. Recently, Mellor (2011) published a paper deriving vertically dependent wave radiation stress terms which are directly related to the equations derived by Longuet-Higgins and Stewart (1964) and Phillips (1977). Instead of neglecting Stokes drift and currents when addressing the problem of wave setup, he extended the equations for three-dimensional flow resulting in:

$$S_{\alpha\beta} = E\left[\frac{k_\alpha k_\beta}{k} e^{2kz} - \delta_{\alpha\beta}\left(ke^{2kz} - \frac{1}{2}\delta(z)\right)\right] \tag{18}$$

Both the Kronecker delta $\delta_{\alpha\beta}$ and the Dirac function $\delta(z)$ are used. In shallow water the equation given by Phillips (1977) can be derived by vertical integration (see Mellor, 2011):

$$\int_{-h}^{\xi} S_{\alpha\beta} dz = E\left[\frac{k_\alpha k_\beta}{k^2}\frac{c_g}{c} + \delta_{\alpha\beta}\left(\frac{c_g}{c} - \frac{1}{2}\right)\right] \tag{19}$$

Here, α and β refer to horizontal coordinates and c_g and c are the group and phase velocity, respectively. The radiation stress can be described as a momentum transport by waves that acts as a horizontal stress (see Holthuijsen, 2007). The gradients in these (shear) stresses act as forces and generate currents (e.g. in the x-direction):

$$F_x = -\frac{\partial S_{xx}}{\partial x} - \frac{\partial S_{xy}}{\partial y} \tag{20}$$

Higher waves will result in higher wave energy and thus generate higher radiation stress gradients. When approaching the coast this effect will contribute to increased current velocities in the coastal area. Especially during a storm event high waves occur and generate strong longshore currents (see Pleskachevsky et al., 2009). Mellor (2003) and Mellor (2008) derived a set of equations that can be utilized as governing equations for an ocean model like FVCOM. In these equations a coupling between waves and currents is achieved by implementing the gradients of radiation stresses as a force acting on the current field. The effect of the current field on the wave is modelled by a shift in wave frequency caused by opposing currents. Thus, the FVCOM model can be used as a combination of the hydrodynamic model FVCOM and the wave model FVCOM-SWAVE to investigate wave-current interaction e.g. at the German coast. The derivation of the wave action equation used in FVCOM-SWAVE is presented in these publications as well.

The North Sea model setup and the Wadden Sea model setup of FVCOM were used to calculate the wave-generated velocities at the East-Frisian Coast. The wave-induced current velocity is calculated by the difference between a model run with and without the wave model coupled to the hydrodynamic model. In figure 5 it can be seen that during the storm period in 2006 the strongest currents were generated with values up to around 0.7 m/s in the North Sea model and around 1.0 m/s in the Wadden Sea model. During 2007 no significant storm surges occurred and the highest longshore currents reached a maximum value of around 0.6 m/s.

The current-wave interaction also influences the surface elevation in the East Frisian Wadden Sea area. The waves produce an increased surface elevation of around 0.15 m in most of the tidal flat area. The overall maximum residual current during the storm event is around 1 m/s during the storm surge Britta in 2006.

6. Wave energy flux

Water particles do not travel with the speed of a propagating wave and stay close to their original position. Therefore, no mass is transported by a traveling wave train. However, energy is transported by a wave in the direction of propagation. In the region of the East Frisian Wadden Sea the chain of barrier islands acts like a natural protection of the north-western German coast and "absorbs" most of the energy. Here, the amount of wave energy or wave energy flux is calculated to estimate the impact on the barrier islands during a storm event and a time period with no significant storms.

The wave energy flux of one wave is defined as the product of energy density and the group velocity of the waves (see Cornett and Zhang, 2008). To take the whole wave train into account this product has to be integrated over all wave frequencies and directions:

$$P = \rho g \int_0^{2\pi}\int_0^{\infty} c_g(f,h) S(f,\Theta_w) df d\Theta_w \tag{21}$$

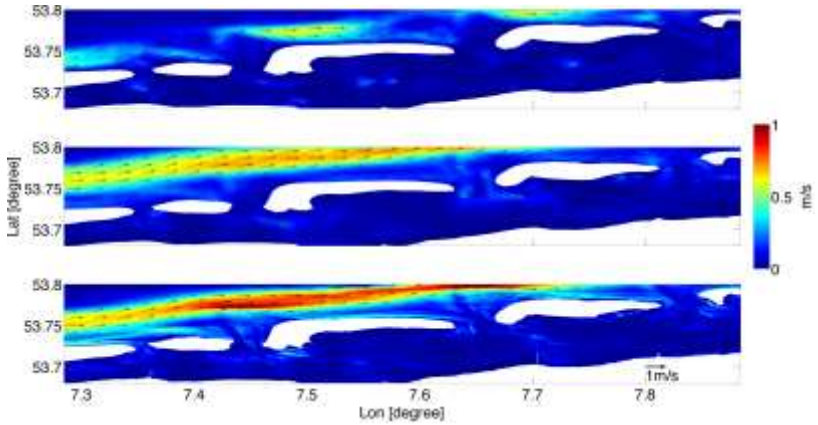

Figure 5. Modelled difference in current velocity due to current-wave interaction. The plot in the top position (North Sea model) shows the difference in current velocity at 18.10.2007, 08:00:00 UTC. The middle (North Sea model) and bottom (Wadden Sea model) plots depict the time point 01.11.06, 01:00:00 UTC during the storm surge Britta. The current velocity is calculated by the difference of two model runs with and without the wave model coupled to the hydrodynamic model. The arrows have been interpolated onto a uniform grid.

Here, S (f,Θ_w) is the 2D wave spectrum, c_g (f, h) the group velocity as already used before, f is the wave frequency and Θ_w the wave direction. The group velocity of every single wave inside a wave train can be calculated as (see Cornett and Zhang, 2008; Holthuijsen, 2007)

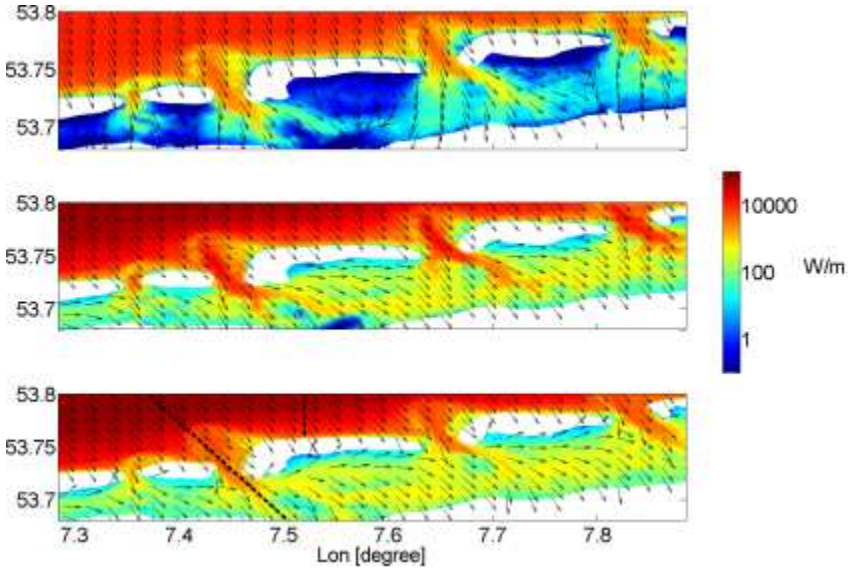

Figure 6. Modelled mean wave energy flux. The figure in the top position (North Sea model) shows the mean wave energy flux during the time period 16.10.07-20.10.07. The middle (North Sea model) and bottom (Wadden Sea model) figures depict the time period 30.10.06-02.11.06 including the storm surge Britta. The arrows have been interpolated onto a uniform grid and normalised to 1.

$$c_g(f,h) = \frac{1}{2}\left[1 + \frac{2kh}{\sinh 2kh}\right]\sqrt{\frac{g}{k}\tanh kh} \tag{22}$$

where kh can be calculated using an approximation given by Fenton and McKee (1990) (see also Holthuijsen, 2007). The wave energy in a wave train can be calculated using the significant wave height

(see Holthuijsen, 2007):

$$E = \frac{1}{16}\rho g H_s^2 \tag{23}$$

Since the energy flux is not yet implemented in the output of the model an approximation of the wave energy flux per unit wave crest length produced by a wave train of irregular waves in any water depth can be estimated from the wave energy (see equation 23), the peak wave period T_p and the local water depth as

$$P \approx \frac{1}{16}\rho g H_s^2 c_g\left(\frac{1}{\alpha_E T_p}, h\right) \tag{24}$$

where $c_g\left(\frac{1}{\alpha_E T_p}, h\right)$ is the group velocity of a wave with a period of $\alpha_E T_p$. The parameter α_E is a coefficient that depends on the shape of the wave spectrum and is shifting the peak period to lower periods. If a sea state is dominated by waves from a single source and the spectrum is uni-modal, Cornett and Zhang (2008) suggest a value of $\alpha_E \approx 0.9$ that was used here.

The resulting mean wave energy flux can be seen in figure 6 for the two different time periods in 2006 and 2007. In 2006, a mean wave energy of about 70 kW/m is approaching the coast. In 2007, less energy is transported by the waves, but in all three cases the barrier islands absorb most of the wave energy. The influence of the ebb-tidal delta in front of the inlet can also be identified.

Figure 7 shows the profile of the maximum daily mean and the mean of wave energy during the time period 30.10.06-02.11.06 interpolated on a section in front of the coast of a barrier island and along a tidal inlet (see figure 6). It can be seen that the maximum daily mean wave energy flux can reach up to 190 kW/m in front of the coast during the storm event, a similar result compared to the value of around 160 kW/m found by Pleskachevsky et al. (2009). In front of the barrier island the wave energy flux shows a strong decrease starting at 4 km before reaching the barrier island Langeoog. Along the tidal inlet it decreases at the area of the ebb-tidal delta rapidly to a value of less than 10 % of the high value in front of the barrier islands like it was mentioned by Krögel and Flemming (1998).

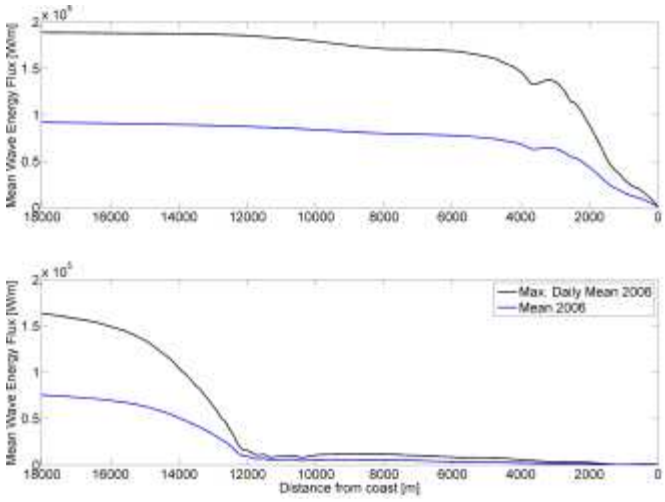

Figure 7. Profile of the mean wave energy flux calculated by the Wadden Sea model. The maximum of daily mean and the mean of wave energy flux during the time period 30.10.06-02.11.06 is shown. The upper plot depicts the section in front of the barrier island Langeoog. The plot at the bottom shows the wave energy flux along a tidal inlet. The position of the sections can be seen in the bottom panel of figure 6.

7. Discussion and concluding remarks

An unstructured-grid ocean model with a North Sea and a Wadden Sea model setup has been tested and

validated for a moderate and a storm situation in 2007 and 2006, respectively. Residual longshore currents that were expected to occur under storm conditions could be reproduced by the model's implemented wave current interaction mechanisms. There haven not been measurements for the longshore current during storm events, so these results are a first approach to estimate the magnitude of this effect in the East Frisian barrier island system. This effect may play a major role in sediment transport and should be a focus of further investigations in future studies. Additionally, a first estimate of the wave-induced energy flux has been calculated, showing a high energy flux under storm conditions and the ability of the barrier island system to absorb most of the energy as it was mentioned by Krögel and Flemming (1998). Some of the energy could also enter the inlet and was dissipated by traveling through the channel, also providing erosion potential in this area. The high resolution Wadden Sea model showed a better performance in predicting the current velocities compared to the coarser North Sea model, indicating energy diffusion in the coarser model. However, the North Sea model setup also reproduced the wave-induced longshore currents. The calculated effects of the wave-current interactions compare well with the results found by Pleskachevsky et al. (2009). The Wadden Sea model setup can be used for the investigation of small-scale processes in the barrier island system of the East Frisian Wadden Sea. Future work should also include long-term runs and the implementation of a variable temperature and salinity distribution in the model setup.

Acknowledgements

The study was supported by the Ministry for Science and Culture of Lower Saxony within the network KLIFF - climate impact and adaption research in Lower Saxony, the initiative Earth Science Knowledge Platform (ESKP) operated by the Helmholtz Association and the North-German Supercomputing Alliance (Norddeutscher Verbund zur Förderung des Hoch- und Höchstleistungsrechnens - HLRN). We thank the developers of the Finite-Volume Coastal Ocean Model (FVCOM) Dr. C. Chen at the University of Massachusetts Dartmouth and Dr. R. Beardsley at the Woods Hole Oceanographic Institution for supplying the source code and initial help.

References

Bartholomä, A., Kubicki A., Badewien T.H., Flemming B.W., 2009. Suspended sediment transport in the German Wadden Sea-seasonal variations and extreme events, *Ocean Dynamics*, 59(2): 213-225.

Booij N., Ris R.C., Holthuijsen L.H., 1999. A third-generation wave model for coastal regions: 1. Model description and validation, *Journal of Geophysical Research*, 104(C4): 7649-7666.

Chen C., Liu H., Beardsley R.C., 2003. An Unstructured Grid, Finite-Volume, Three-Dimensional, Primitive Equations Ocean Model: Application to Coastal Ocean and Estuaries, *Journal of Atmospheric and Oceanic Technology*, 20(1): 159-186.

Chen C., Beardsley R.C., Cowles G., 2006. *An Unstructured Grid, Finite-Volume Coastal Ocean Model, FVCOM User Manual 2nd edn. SMAST/UMASSD Tech. Rep. 06-0602, 315 pp*, School for Marine Science and Technology, University of Massachusetts-Dartmouth, New Bedford, MA.

Cornett A. and Zhang J., 2008. *Nearshore Wave Energy Resources, Western Vancouver Island, B.C., Technical Report CHC-TR-51*, Canadian Hydraulics Centre.

Dastgheib A., Roelvink J.A., Wang Z.B., 2008. Long-term process-based morphological modeling of the Marsdiep Tidal Basin, *Marine Geology*, 256(1-4): 90-100.

Fenton J.D. and McKee W.D., 1990. On calculating the lengths of water waves, *Coastal Engineering*, 14(6): 499-513.

Flemming B.W. and Bartholomä, A., 1997. Response of the Wadden Sea to a Rising Sea Level: a Predictive Empirical Model, *Deutsche Hydrographische Zeitschrift*, 49(2-3): 343-353.

Geuzaine C. and Remacle J.F., 2009. GMSH: a three-dimensional finite element mesh generator with built-in pre- and postprocessing facilities, *International Journal for Numerical Methods in Engineering*, 79(11): 1309-1331.

Holthuijsen L.H., 2007. *Waves in Oceanic and Coastal Waters*, Cambridge University Press.

Kliem N., Nielsen J.W., Huess V., 2006. Evaluation of a shallow water unstructured mesh model for the North Sea Baltic Sea, *Ocean Modelling*, 15(1-2): 124-136.

Krögel F. and Flemming B.W., 1998. Evidence for temperature-adjusted sediment contributions in the back-barrier tidal flats of the East Frisian Wadden Sea (southern North Sea), *In: Alexander, CR et al. (eds.) (1998) Tidalites: processes & products. SEPM Special Publication no. 61. SEPM, Tulsa*, pp. 31-41.

Lettmann K.A., Wolff J.-O., Badewien T.H., 2009. Modeling the impact of wind and waves on suspended particulate matter fluxes in the East Frisian Wadden Sea (southern North Sea), *Ocean Dynamics*, 59(2): 239-262.

Loewe P (2009) *System Nordsee - Zustand 2005 im Kontext langzeitlicher Entwicklungen*, Berichte des Bundesamtes für Seeschifffahrt und Hydrographie 44.
Longuet-Higgins M.S. and Stewart R.W., 1964. Radiation stresses in water waves; a physical discussion with applications, *Deep-Sea Research*, 11:529-562.
Longuet-Higgins M.S., 1970. Longshore current generated by obliquely incident sea waves, 1, *Journal of Geophysical Research*, 75(33): 6778-6789.
Lyard F., Lefevre F., Letellier T., Francis O., 2006. Modelling the global ocean tides: modern insights from FES2004, *Ocean Dynamics*, 56(5-6): 394-415.
Mellor G., 2003. The Three-Dimensional Current and Surface Wave Equations, *Journal of Physical Oceanography*, 33(9): 1978-1989.
Mellor G., 2005. Some Consequences of the Three-Dimensional Current and Surface Equations, *Journal of Physical Oceanography*, 35(11): 2291-2298.
Mellor G.L., 2008. The Depth-Dependent Current and Wave Interaction Equations: A Revision, *Journal of Physical Oceanography*, 38(11): 2587-2596.
Mellor G., 2011. Wave radiation stress, *Ocean Dynamics*, 61(5): 563-568.
Mellor G.L. and Yamada T., 1982. Development of a Turbulence Closure Model for Geophysical Fluid Problems, *Reviews of Geophysics*, 20(4): 851-875.
Osuna P. and Monbaliu J., 2004. Wave-current interaction in the Southern North Sea, *Journal of Marine Science*, 52(1-4): 65-87.
Phillips O.M., 1977. *The dynamics of the upper ocean*, Cambridge University Press
Pleskachevsky A., Eppel D.P., Kapitza H., 2009. Interaction of waves, currents and tides, and wave-energy impact on the beach area of Sylt Island, *Ocean Dynamics*, 59(3): 451-461.
Qi J., Chen C., Beardsley R.C., Perry W., Cowles G.W., Lai Z., 2009. An unstructured-grid finite-volume surface wave model (FVCOM-SWAVE): Implementation, validations and applications, *Ocean Modelling*, 28(1-3): 153-166.
Reuter R., Badewien T.H., Bartholomä A., Braun, A., Lübben A., Rullkötter J., 2009. A hydrographic time series station in the Wadden Sea (southern North Sea), *Ocean Dynamics*, 59(2): 195-211.
Santamarina Cuneo P. and Flemming B.W., 2000. Quantifying concentration and flux of suspended particulate matter through a tidal inlet of the East Frisian Wadden Sea by acoustic Doppler current profiling, *In: Flemming, BW et al.* (eds.) (2000) Muddy Coast Dynamics and Resource Management. Proceedings in Marine Science vol. 2. Elsevier, *Amsterdam*, pp. 39-52.
Stanev E.V., Wolff J.-O., Burchard H., Bolding K., Flöser G., 2003a. On the circulation in the East Frisian Wadden Sea: numerical modeling and data analysis, *Ocean Dynamics*, 53(1): 27-51.
Stanev E.V., Flöser G., Wolff J.-O., 2003b. First- and higher-order dynamical controls on water exchanges between tidal basins and the open ocean. A case study for the East Frisian Wadden Sea, *Ocean Dynamics*, 53(3): 146-165.
Stanev E.V., Wolff J.-O., Brink-Spalink G., 2006. On the sensitivity of the sedimentary system in the East Frisian Wadden Sea to sea-level rise and wave-induced bed shear stress, *Ocean Dynamics*, 56(3-4): 266-283.
Stanev E.V., Flemming B.W., Bartholomä, A., Staneva, J.V., Wolff J.-O., 2007a. Vertical circulation in shallow tidal inlets and back-barrier basins, *Continental Shelf Research*, 27(6): 798-831.
Stanev E.V., Brink-Spalink G., Wolff, J.-O., 2007b. Sediment dynamics in tidally dominated environments controlled by transport and turbulence: A case study for the East Frisian Wadden Sea, *Journal of Geophysical Research*, 112(C4)
Staneva J., Stanev E.V., Wolff J.-O., Badewien T.H., Reuter R., Flemming B., Bartholomä A., Bolding K., 2009. Hydrodynamics and sediment dynamics in the German Bight. A focus on observations and numerical modelling in the East Frisian Wadden Sea, *Continental Shelf Research*, 29(1): 302-319.
Smagorinsky J., 1963. General circulation experiments with the primitive equations I. The basic experiment, *Monthly Weather Review*, 91(3): 99-164.
Thornton E.B. and Guza R.T., 1986. Surf Zone Longshore Currents and Random Waves: Field Data and Models, *Journal of Physical Oceanography*, 16(7): 1165-1178.
Wang Z.B., Hoekstra P., Burchard H., Ridderinkhof H., De Swart H.E., Stive M.J.F., 2012. Morphodynamics of the Wadden Sea and its barrier island system, *Ocean & Coastal Management*, 68: 39-57.
Van der Wegen, M., Dastgheib, A., Roelvink, J.A., 2010. Morphodynamic modeling of tidal channel evolution in comparison to empirical PA relationship, *Coastal Engineering*, 57(9): 827-837.
Weisse R., von Storch H., Niemeyer H.D., Knaack H., 2011. Changing North Sea storm surge climate: An increasing hazard? *Ocean & Coastal Management*, 68: 58-68.
Wu, L., Chen C., Guo P., Shi M., Qi J., Ge J., 2011. A FVCOM-Based Unstructured Grid Wave, Current, Sediment Transport Model, I. Model Description and Validation, *Journal of Ocean University of China*, 10(1): 1-8.
Yu Q., Wang Y., Flemming B., Gao S., 2012. Modelling the equilibrium hypsometry of back-barrier tidal flats in the German Wadden Sea (southern North Sea), *Continental Shelf Research*, 49: 90-99.